

Structure Analysis of the Si(111) $\sqrt{3}\times\sqrt{3}R30^\circ$ -Ag Surface

M. Katayama,⁽¹⁾ R. S. Williams,⁽²⁾ M. Kato,⁽³⁾ E. Nomura,⁽⁴⁾ and M. Aono^{(1),(4)}

⁽¹⁾Surface and Interface Laboratory, RIKEN Institute, Wako-shi, Saitama 351, Japan

⁽²⁾Department of Chemistry and Biochemistry, University of California, Los Angeles, California 90024

⁽³⁾Department of Physics, Ehime University, Matsuyama, Ehime 790, Japan

⁽⁴⁾Aono Atomcraft Project, Kaga 1-7-13, Itabashi, Tokyo 173, Japan

(Received 9 July 1990)

The structure of the Si(111) $\sqrt{3}\times\sqrt{3}R30^\circ$ -Ag surface has been analyzed with a novel form of low-energy ion-scattering spectroscopy and energy-minimization calculations. The topmost layer of the surface is formed by Ag atoms with a honeycomb-chained-trimer arrangement in which the intratrimer Ag-Ag distance is 5.1 ± 0.2 Å. At 0.75 ± 0.07 Å below the Ag layer, there exists a Si layer with three Si atoms per surface unit cell. The lower layer of the subsequent bulklike Si double layers is split into a honeycomb and a $\sqrt{3}\times\sqrt{3}$ layer with a large interlayer distance of about 0.6 Å.

PACS numbers: 68.35.Bs, 61.16.Fk

The structural analysis of the Si(111) $\sqrt{3}\times\sqrt{3}R30^\circ$ -Ag surface ($\sqrt{3}\times\sqrt{3}$ surface) has been one of the important pending problems in surface science. Since the first study¹ on this surface was reported more than twenty years ago, almost all surface-sensitive experimental methods have been employed to analyze its structure, and a number of structural models have been proposed, i.e., simple honeycomb (HC),²⁻⁵ missing top layer (MTL),^{4,6-9} embedded honeycomb (EHC),¹⁰⁻¹² atop trimer (AT),¹³ substitutional trimer (ST),¹⁴⁻¹⁹ honeycomb-chained-trimer (HCT),²⁰⁻²³ centered hexagon (CH),²⁴ silicon-adatom-vacancy (SAV),²⁵ and silver-honeycomb-chained-trimer²⁶ (SHCT) models. However, none of these models is universally accepted as being correct. Indeed, two scanning-tunneling-microscopy studies^{4,5,18,19} have yielded completely different models, and two x-ray-diffraction studies^{20,23,26} have also resulted in different models. Most researchers agree that the $\sqrt{3}\times\sqrt{3}$ unit cell contains three Ag atoms,^{10,13,25,27,28} although whether the Ag atoms form the topmost layer or are embedded below a Si layer is still controversial. In this paper, we show that our clear-cut experimental re-

sults from low-energy ion-scattering spectroscopy, combined with energy-minimization calculations, yield a modified HCT model, which is consistent with most of the reported experimental results.

The low-energy ion-scattering spectroscopy experiments were done in the mode of coaxial impact-collision ion-scattering spectroscopy (CAICISS),^{29,30} in which an ion source and a time-of-flight (TOF) energy analyzer are placed coaxially so as to put the experimental scattering angle at 180° ($\pm 1.5^\circ$). The most striking characteristic of this mode is that the center of each atom is "seen" via a head-on collision with an ion, which makes data analysis simple. All the CAICISS experiments were done with an incident beam of 2-keV He⁺. The $\sqrt{3}\times\sqrt{3}$ surface was prepared in the usual method described elsewhere.³¹ All computer simulations of ion scattering in this paper were carried out using a multi-target cross-section calculation.³²

Shown in Fig. 1 are selected CAICISS energy spectra of the $\sqrt{3}\times\sqrt{3}$ surface, which were measured as a function of the azimuthal angle about the sample normal, ϕ , at 1° intervals, with the angle between the axis and the

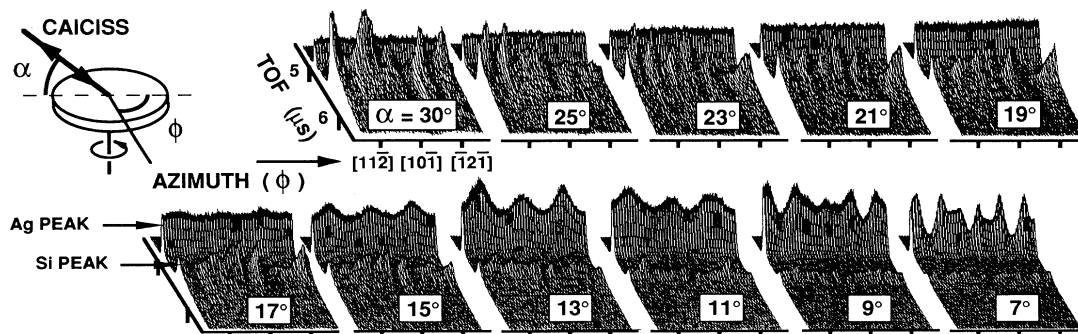


FIG. 1. CAICISS spectra of the $\sqrt{3}\times\sqrt{3}$ surface, measured by changing ϕ at 1° intervals, α being fixed at various values (see the inset for α and ϕ).

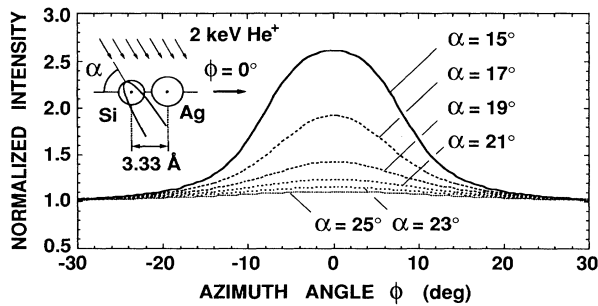


FIG. 2. Computer simulations of the intensity of He particles scattered from the Ag atom of an Ag-Si pair parallel to the surface as a function of ϕ at various α 's for an incident beam of 2-keV He^+ (see the inset for α and ϕ).

surface plane, α , being fixed at various values. Peaks at TOF of 4.83 and 5.35 μs are caused by He particles (He^+ and He^0) scattered from Ag and Si atoms, respectively (referred to as the Ag peak and the Si peak, respectively); scattered He^+ and He^0 are both detected in CAICISS, so that there is no ambiguity related to the neutralization probability of incident He^+ . An important feature of Fig. 1 is that the intensity of the Ag peak, I_{Ag} , is constant, being independent of ϕ for $\alpha > 19^\circ$, and shows noticeable variations only for $\alpha < 17^\circ$. This clearly indicates that the Ag atoms form the topmost layer, as will be discussed below.

The inset of Fig. 2 shows neighboring Si and Ag atoms at an imaginary surface. Computer simulations were carried out for the intensity of He particles scattered from the Ag atom with changing ϕ at various α 's for an incident beam of 2-keV He^+ , as shown in Fig. 2. In the simulations, the Ag and Si atoms were at the same height and the lateral distance between the two atoms was 3.33 \AA , which is the possible maximum Ag-Si lateral distance under the condition that the $\sqrt{3} \times \sqrt{3}$ unit cell contains three Ag atoms. As we see in Fig. 2, the intensity shows strong variations with ϕ , which are caused by shadowing (the Ag atom is shadowed by the Si atom) and focusing (the Ag atom is bathed in a focused ion flux due to the existence of the Si atom), even at values of α as large as 21° ; if the Ag-Si distance is decreased from 3.33 \AA to a more realistic value, 2.61 \AA , which is the sum of the atomic radii of Ag and Si, the intensity variations become much stronger. If we compare Fig. 2 with the experimental results in Fig. 1, where I_{Ag} shows no variation at all with ϕ for $\alpha > 19^\circ$, it is obvious that the Ag atoms are not embedded below any Si layer, but are exposed, forming the topmost layer.

In order to analyze the lateral arrangement of the topmost Ag atoms, I_{Ag} was measured as a function of α in the $[\bar{1}10]$ and $[\bar{1}\bar{1}2]$ azimuths, as shown in Fig. 3(a). Corresponding computer simulations were made for a number of different lateral arrangements of Ag atoms and it was found that only the HCT arrangement was

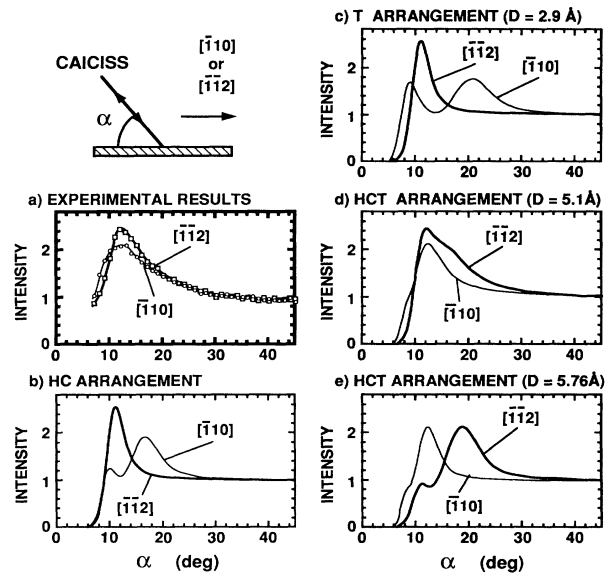


FIG. 3. (a) The intensity of He particles scattered from Ag atoms of the $\sqrt{3} \times \sqrt{3}$ surface measured as a function of α along the $[\bar{1}10]$ and $[\bar{1}\bar{1}2]$ azimuths (see the inset for α). (b)–(e) Computer simulations for various arrangements of Ag atoms.

consistent with the experimental results. As an example of inconsistent cases, the results for the HC arrangement are shown in Fig. 3(b), which clearly disagree with the experimental results. Even in the case of the HCT arrangement, good agreement is obtained only when the intratrimer Ag-Ag distance D is $5.1 \pm 0.2 \text{\AA}$, as shown in Fig. 3(d) (the disagreement observed at small α 's is not serious because this is caused by surface imperfections such as atomic steps and vacancies); if D is increased or decreased from $5.1 \pm 0.2 \text{\AA}$, a disagreement is seen, as shown in Figs. 3(c) and 3(e) [the case of $D = 2.9 \text{\AA}$, Fig. 3(c), coincides with the T arrangement]. The HCT ar-

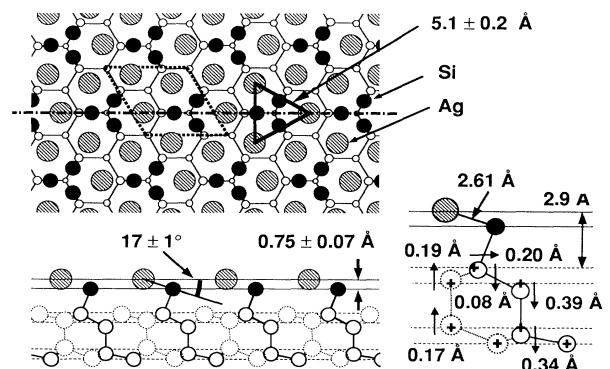


FIG. 4. Modified HCT model for the structure of the $\sqrt{3} \times \sqrt{3}$ surface, which is derived from the CAICISS experiments with the aid of energy-minimization calculations.

arrangement of Ag atoms with $D = 5.1 \pm 0.2 \text{ \AA}$ is illustrated in Fig. 4, which shows our modified HCT model for the $\sqrt{3} \times \sqrt{3}$ structure discussed later. This arrangement of Ag atoms is also consistent with the ϕ dependence of I_{Ag} seen in Fig. 1 with respect to the angular positions of the observed shadowing dips.

Figure 5 shows a CAICISS spectrum of the $\sqrt{3} \times \sqrt{3}$ surface, which was measured by taking the CAICISS axis normal to the surface. Shown in the insets (a)–(h) are various scattering trajectories of He^+ in the geometry of CAICISS, or 180° total (experimental) scattering angle. A striking characteristic of the 180° total scattering angle is that double scattering by two atoms of the same mass and single scattering by an atom of that kind give the same postscattering kinetic energy regardless of the orientation of the two atoms. Because of this, trajectories (a) and (b) related to the Ag atoms give a single peak at a TOF of $4.83 \mu\text{s}$ and trajectories (f)–(h) related to Si atoms give a single peak at a TOF of $5.35 \mu\text{s}$ (referred to as the Ag peak and the Si peak as before), although the contribution (cross section) of double scattering is much smaller than that of single scattering (less than 6%). On the other hand, trajectories (c)–(e), which are related to both Ag and Si atoms, yield a spectral peak between the Ag peak and the Si peak. The position of the peak depends on the angle between the Ag-Si axis and the surface plane β , where β is defined to be positive (negative) when the Ag atom is higher (lower) than the Si atom. In particular, if $\beta = 0$, the peak appears at a position indicated by the thick vertical line in Fig. 5, and if $\beta > 0$ ($\beta < 0$), the peak appears on the larger- (smaller-) TOF side. As we see in Fig. 5, such a peak is not observed on the smaller-TOF side, but there

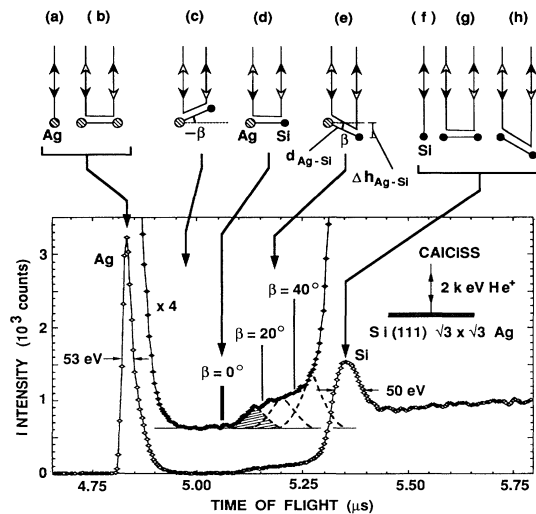


FIG. 5. CAICISS spectrum of the $\sqrt{3} \times \sqrt{3}$ surface measured with the axis of CAICISS normal to the surface. Insets (a)–(h): Various trajectories for ion scattering and the positions in the spectrum where they should be detected.

is a distinct structure on the larger-TOF side. This also clearly shows that the Ag atoms form the topmost layer (see Fig. 4). The reason why the observed structure is not a peak but a broad plateau is that there are many Ag-Si pairs with different β 's. In other words, the observed broad structure contains information on the distribution of the underlying Si atoms, as will be discussed below.

By taking the total-energy resolution of our instrument (about 50 eV) as well as the discussions given below into account, the broad plateau is divided into substructures as shown by the broken curves in Fig. 5. The leading substructure, indicated by hatching, corresponds to the smallest β and is related to Si atoms in a Si layer next to the topmost Ag layer (see Fig. 4). Other substructures, which correspond to larger β 's, are related to Si atoms in the subsequent bulklike Si double layers (see Fig. 4). From the position of the leading substructure, TOF of $5.14 \pm 0.01 \mu\text{s}$, we calculate that β for the Ag-Si pairs related to the Si layer next to the topmost Ag layer is $17^\circ \pm 1^\circ$ (see Fig. 4). Therefore, if the interatomic distance of the Ag-Si pair, $d_{\text{Ag-Si}}$, is given, $\Delta h_{\text{Ag-Si}}$ can be estimated. In the various structural models^{1–26} of the $\sqrt{3} \times \sqrt{3}$ surface, $d_{\text{Ag-Si}}$ is distributed between 2.48 and 2.63 \AA . This corresponds to $\Delta h_{\text{Ag-Si}} = 0.75 \pm 0.07 \text{ \AA}$ (see Fig. 4). From the intensity of the leading substructure relative to that of the Ag peak, we can estimate the number density of Si atoms in the Si layer next to the topmost Ag layer by calculating and comparing the cross sections for the scattering trajectories shown in insets (a), (b), and (e) of Fig. 5. The number density is estimated to be about three per $\sqrt{3} \times \sqrt{3}$ cell (see Fig. 4), in accordance with x-ray-diffraction^{23,26} and electron-diffraction²¹ experiments, so that this Si layer will be referred to as the Si trimer layer.

In Fig. 4, the bond between a Si atom in the Si trimer layer and its nearest-neighbor bulklike Si atom is tilted from the surface normal. It is therefore expected that subsurface bulklike Si atoms are relaxed from their ideal positions. The magnitude of the relaxation of each bulklike Si atom was estimated by energy-minimization calculations using the Keating method³³ (the Si atoms in the Si trimer layer and those in the fourth bulklike Si layer were fixed at the experimental and ideal positions, respectively) and the results are shown in Fig. 4. As we see, the second bulklike Si layer is split into two layers with a large interlayer distance of about 0.6 \AA resulting in a honeycomb layer and a $\sqrt{3} \times \sqrt{3}$ layer. In x-ray-diffraction^{23,26} and electron-diffraction²¹ studies of the $\sqrt{3} \times \sqrt{3}$ surface, the existence of a Si honeycomb layer has been suggested in order to obtain a better reliability factor in the data analysis. Our structural model, Fig. 4, indeed contains such a Si honeycomb layer.

Recently, Watanabe *et al.*³⁴ performed energy-band calculations for our structural model, Fig. 4, using the density-functional method. The results agree very well

with reported photoemission³⁵ and inverse photoemission³⁶ data in regard to the band gap, the energy positions of Ag 4*d* bands, and the density-of-states profiles of both filled and empty bands.

To summarize, we have proposed a new structural model, a modified HCT model, for the Si(111) $\sqrt{3} \times \sqrt{3}R30^\circ$ -Ag surface on the basis of CAICISS experiments and energy-minimization calculations. The model is consistent with most of reported experimental results.

- ¹K. Spiegel, Surf. Sci. **7**, 125 (1967).
²G. Le Lay, Surf. Sci. **132**, 169 (1983).
³M. Aono, R. Souda, C. Oshima, and Y. Ishizawa, Surf. Sci. **168**, 713 (1986).
⁴R. J. Wilson and S. Chaing, Phys. Rev. Lett. **59**, 2329 (1987).
⁵R. J. Wilson and S. Chaing, Phys. Rev. Lett. **58**, 369 (1987).
⁶E. L. Bullock, G. S. Herman, M. Yamada, D. J. Friedman, and C. S. Fadley, Phys. Rev. B **41**, 1703 (1990).
⁷S. Kono, K. Higashiyama, and T. Sagawa, Surf. Sci. **165**, 21 (1986).
⁸S. Kono, H. Sakurai, K. Higashiyama, and T. Sagawa, Surf. Sci. **130**, L299 (1983).
⁹S. Kono, K. Higashiyama, T. Kinoshita, T. Miyahara, H. Kato, H. Ohsawa, Y. Enta, F. Maeda, and Y. Yaegashi, Phys. Rev. Lett. **58**, 1555 (1987).
¹⁰M. Saitoh, F. Shoji, K. Oura, and T. Hanawa, Surf. Sci. **112**, 306 (1981).
¹¹Y. Terada, T. Yoshizauka, K. Oura, and T. Hanawa, Surf. Sci. **114**, 65 (1982).
¹²J. Stöhr, R. Jaeger, G. Rossi, T. Kendelewicz, and I. Lindau, Surf. Sci. **134**, 813 (1983).
¹³F. Wehking, H. Beckermann, and R. Niedermayer, Surf. Sci. **71**, 364 (1978).
¹⁴Y. Horio and A. Ichimiya, Surf. Sci. **164**, 589 (1985).
¹⁵C. S. Chang, T. L. Porter, and I. S. T. Tsong, J. Vac. Sci. Technol. B **3**, 1906 (1988).
¹⁶T. L. Porter, C. S. Chang, and I. S. T. Tsong, Phys. Rev. Lett. **60**, 1739 (1988).
¹⁷Y. Horio and A. Ichimiya, Surf. Sci. **133**, 393 (1983).
¹⁸J. E. Demuth, E. J. Van Loenen, R. M. Tromp, and R. J. Hamers, J. Vac. Sci. Technol. B **6**, 18 (1988).
¹⁹E. J. Van Loenen, J. E. Demuth, R. M. Tromp, and R. J. Hamers, Phys. Rev. Lett. **58**, 373 (1987).
²⁰T. Takahashi, S. Nakatani, N. Okamoto, T. Ichikawa, and S. Kikuta, Jpn. J. Appl. Phys. **27**, L753 (1988).
²¹A. Ichimiya, S. Kohmoto, T. Fujii, and Y. Horio, Appl. Surf. Sci. **41/42**, 82 (1989).
²²R. S. Williams, R. S. Daley, J. H. Huang, and R. M. Charatan, Appl. Surf. Sci. **41/42**, 70 (1988); R. S. Daley, R. M. Charatan and R. S. Williams, Surf. Sci. **240**, 136 (1990).
²³T. Takahashi, in Proceedings of the Workshop on the Si(111) $\sqrt{3} \times \sqrt{3}$ -Ag Surface, Tokyo, 3 January 1989 (unpublished).
²⁴G. Le Lay, A. Chauvet, M. Manneville, and R. Kern, Surf. Sci. **9**, 190 (1981).
²⁵M. Copel and R. M. Tromp, Phys. Rev. B **39**, 12688 (1989).
²⁶E. Vlieg, A. W. van der Gon, J. F. van der Veen, J. E. MacDonald, and C. Norris, Surf. Sci. **209**, 100 (1989).
²⁷E. J. Van Loenen, M. Iwami, R. M. Tromp, and J. F. van der Veen, Surf. Sci. **137**, 1 (1984).
²⁸J. A. Venables, J. Derrin, and A. P. Janssen, Surf. Sci. **95**, 411 (1980).
²⁹M. Katayama, E. Nomura, N. Kanekama, H. Soejima, and M. Aono, Nucl. Instrum. Methods Phys. Res., Sect. B **33**, 857 (1988).
³⁰M. Aono, M. Katayama, E. Nomura, T. Chasse, D. Choi, and M. Kato, Nucl. Instrum. Methods Phys. Res., Sect. B **37/38**, 264 (1989).
³¹I. Kamiya, M. Katayama, E. Nomura, and M. Aono, Surf. Sci. (to be published).
³²R. S. Williams, M. Kato, R. S. Daley, and M. Aono, Surf. Sci. **225**, 355 (1990).
³³P. N. Keating, Phys. Rev. **145**, 637 (1966).
³⁴S. Watanabe, M. Tsukada, K. Katayama, M. Kato, and M. Aono, in Proceedings of the Extended Abstracts of the Spring Meeting of the Physical Society of Japan, March 1991 (to be published).
³⁵T. Yokotsuka, S. Kono, S. Suzuki, and T. Sagawa, Surf. Sci. **127**, 35 (1983).
³⁶J. M. Nicholls, F. Salvan, and B. Reihl, Phys. Rev. B **34**, 2945 (1986).